Development of laser-produced plasma based EUV light source technology for HVM EUV lithography

Junichi Fujimoto, Tsukasa Hori*, Tatsuya Yanagida*, Takeshi Ohta*, Yasufumi Kawasuji*,
Yutaka Shiraishi*, Tamotsu Abe*, Takeshi Kodama*,
Hiroaki Nakarai*, Taku Yamazaki* and Hakaru Mizoguchi

Gigaphoton Inc. 400 Yokokurashinden Oyama-shi Tochigi-ken 323-8558, JAPAN
*KOMATSU Ltd. 3-25-1 Shinomiya Hiratsuka-shi Kanagawa-ken 254-8555, JAPAN

ABSTRACT

Since 2002, we have been developing a CO_2-Sn-LPP EUV light source, which is the most promising solution as the 13.5 nm high power (>200 W) light source for HVM EUVL for its high efficiency, power scalability, and spatial freedom around plasma. We believe that the CO_2-Sn-LPP scheme is the most feasible candidate for the EUV light source for HVM. We have several engineering data from our test tools, which include: the maximum of 3.8 % CE, the maximum of 2.5 mJ pulse energy, 93 % Sn ionization rate, 98 % Sn debris mitigation by a magnetic field, and 68 % CO_2 laser energy absorption rate. Based on these data we are developing our first light source for HVM: "GL200E." The latest data and the overview of EUV light source for the HVM EUVL are reviewed in this paper. Part of this work was supported by the New Energy and Industrial Technology Development Organization (NEDO).

Keywords: EUV light source, laser produced plasma, CO_2 laser, EUV, Lithography

1. INTRODUCTION

Since 2002, Gigaphoton/Komatsu have been developing a laser plasma produced (LPP) EUV light source based upon carbon dioxide (CO_2) laser produced Tin (Sn) plasma,

The CO_2-Sn-LPP EUV light source is deemed to be the most promising solution as the 13.5 nm high power (>200 W) light source for HVM EUV lithography (EUVL) [1, 2, 3, 4] because of the high efficiency, power scalability, and spatial freedom around plasma. Therefore, we have chosen the LPP-EUV method. We believe that the CO_2-Sn-LPP scheme is the most feasible candidate for the EUV light source for HVM.

In order to meet the performance requirements for an EUV light source, We have focused on three enabling technologies:

1. high conversion efficiency (CE)
2. debris mitigation functionality
3. CO_2 laser power usage

We have investigated how Sn droplets under laser irradiation generate EUV light. Also investigated is Sn behavior, in vacuum environment, under irradiation of laser beams.

In this paper, we report on the present development status of our LPP light source for EUVL for HVM.

2. LPP EUV LIGHT SOURCE EQUIPMENT CONFIGURATIONS

The typical setup of an EUV light source system is shown in Figure 1.

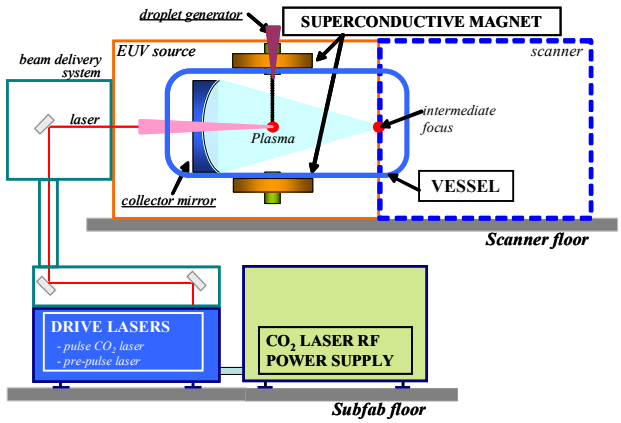

Figure 1: Typical layout of a LPP EUV light source

Our EUV light source contains, four primary sections:

1. EUV vessel including droplet generator and collector mirror
2. Superconductive magnets for debris mitigation
3. Plasma generation drive lasers, composed of pre-pulse laser and pulsed CO_2 laser
4. CO_2 laser power supply system

We are developing LPP-EUV light source based upon an experimental system. The small experimental tool is employed for Sn target shooting optimization. The features of this system are shown below. The GL200E proto system is used for system performance demonstration. Our target is to develop the GL200E system, which will be our first generation HVM EUV light source based upon the GL200E proto system.

2.1 Small experimental light source tool (Figure 2)

We have investigated EUV plasma generation scheme with the use of the small experimental tool operated at the repetition rate of 10 Hz (maximum). Figure 2 shows the experimental setup for the basic investigation of EUV light generation and Sn debris mitigation [5, 6].

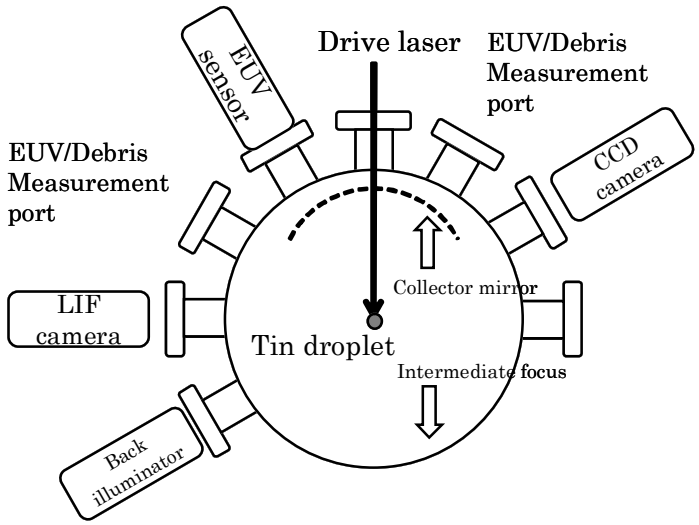

Figure 2: Diagram of small experimental tool

The small experimental light source setup simulates the final system, except for the repetition rate of the driver laser and can be operated with and without magnetic field applied. It can simulate a 20 kW CO_2 laser with pulse energy of 200 mJ/pulse at low repetition rate of less than 10 Hz. The setup has various diagnostic features where Sn can be observed throughout the entire process from droplet generation to EUV plasma generation.

This tool is capable of simulating conditions of EUV light generation identical to those in GL200E, such as pulse duration, pulse energy of CO_2 laser, pre-pulse laser, Sn droplet size, and magnetic field environment with the only significant difference that it operates at a maximum repetition rate of 10Hz. The tool's compactness makes it easier to measure results and optimize various plasma generation parameters. The small experimental tool consists of various sub systems, including, a short-pulsed high-energy CO_2 laser, a pre-pulse laser, a Sn droplet generator, and a EUV vacuum vessel with a solenoid magnet. By using this tool, we are able to investigate EUV light emission under sequential pre-pulse laser and a CO_2 laser irradiation conditions. The development purpose for small experimental system is primarily debris mitigation analysis, Sn droplet and plasma formation and CO_2 laser energy consumption budget experiments.

2.3 GL200E proto system (Figure 3)

The prototype system of our first high volume manufacturing (HVM) EUV light source has a 100 kHz 20 kW CO_2 laser, 20 μm in diameter droplet generator, and magnetic field debris mitigation functionality.

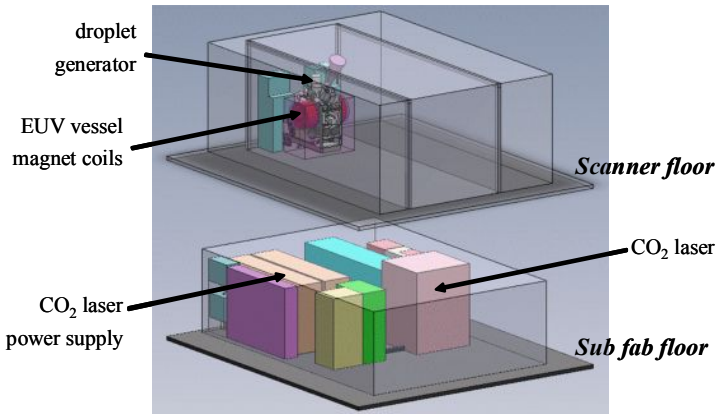

Figure 3: LPP EUV source system layout; Gigaphoton GL200E

The development purpose for the GL200E proto system is integration of all functionalities, testing and debugging based upon a HVM configured EUV light source. This system is planned to be integrated to a scanner system and to demonstrate actual lithographic performance. The target system specifications are shown in Table 1. The HVM system is required to balance many key performance aspects, such as: reliability, maintainability, footprint compactness and affordable operational cost.

Table 1: Target specification of EUV source, GL200E for HVM

Model #	units	Gigaphoton GL200E
EUV Clean Power (@I/F)	W	250 [in-band; after filtering IR & DUV]
EUV Pulse energy (@I/F)	mJ	~ 2.5
Max. Rep. Rate	kHz	~ 100
Max. CO_2 laser system	kW	20 [100 kHz, 200 mJ/pulse]
Target material and shape		Liquid Sn droplet, spherical
Droplet size (diameter)	μm	10 - 30
Plasma creation scheme		Double pulse laser shooting
Debris mitigation scheme		Hybrid; magnetic field guiding & chemical etching

3. ENABLING FUNCTIONS TO MEET EUV LIGHT SOURCE PERFORMANCE

There are three high level performance requirements necessary to be realized in order for LPP-EUV light source to be successful in the industry, high clean EUV power and EUV source reliability/availability for high volume continuous fab operation. In this section, we will discuss and demonstrate the three major enabling functionalities we are developing, in order to achieve the necessary performance.
The three enabling functionalities are:

1. High CE
2. Effective debris mitigation
3. Efficient CO_2 laser energy consumption

Each function will be discussed at length in the following sections.

3.1 High CE

When a Sn droplet target is irradiated with a pre-pulse laser beam and/or a CO_2 laser beam, the Sn droplet in the vessel is converted into a plasma emitting EUV where several states of Sn exist simultaneously. Sn present during plasma generation is generally classified in three categories: fragments, neutral atoms, or ions. After emitting EUV light residues of the plasma are eventually scattered inside the vessel. To prevent the collector mirror from being contaminated, Sn debris needs to be trapped before being deposited onto the collector mirror surface or cleaned after deposition. This Sn-state scheme is shown in Figure 4.

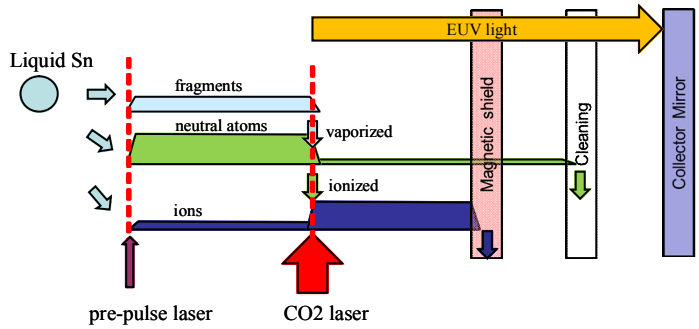

Figure 4: Droplet to Sn debris mitigation concept

To enhance EUV energy and to minimize Sn debris towards the collector, the ionization of the Sn should be maximized in the laser irradiation processes. We believe the shape of the Sn target is crucial. To realize this, a double laser irradiation process is utilized in our system. The theoretical [7] and experimental [8] data have clearly demonstrated the advantage of combining a laser beam at a wavelength of a CO_2 laser with Sn plasma to achieve high CE from driver laser pulse energy to EUV in-band energy [9].

We have reported previously that the Sn fragments are generated during the pre-pulse irradiation [7]. The Sn fragments are, at that moment, the majority of the Sn present. Fragments can reach a maximum of a few micrometers in diameter. The Sn fragments were measured by a shadowgraph method. Figure 5 shows the shadowgraphs of the fragments after the pre-pulse laser irradiation for the droplet with 20 μm diameter. The droplet is irradiated by a pre-pulse laser originating from left hand side in the image.

During laser irradiation, the Sn droplet is displaced away from the irradiation point while simultaneously expanding in diameter. Figure 5 e) shows the images after the pre-pulse laser irradiation without the main CO_2 laser irradiation. Figure 5 c) shows the images with the main CO_2 laser irradiation. Figure 5 d) is captured immediately after the EUV light emission. When irradiation condition is optimized, the fragments have disappeared from the shadowgraph image.

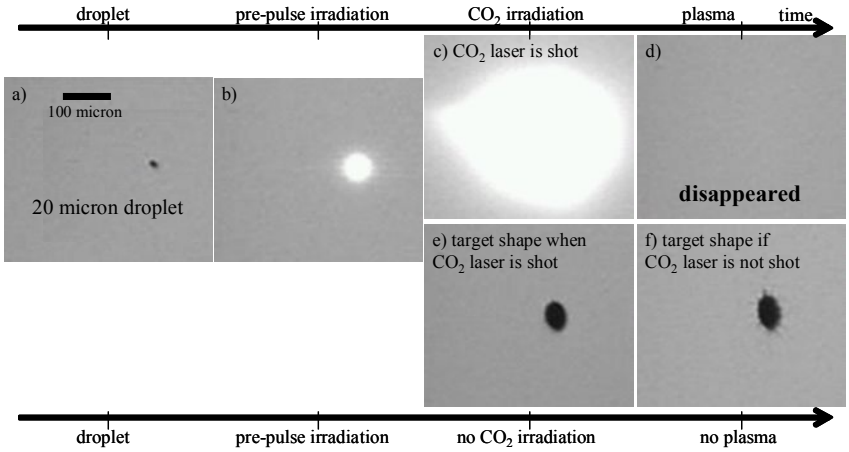

Figure 5: Shadowgraph images of the Sn fragments

The CE with the droplet target is measured. A CE of 3.5 %, using 20 μm diameter droplet and 200 mJ CO_2 laser irradiation, has been demonstrated by optimizing the pre-pulse laser conditions as shown in Figure 6. We also have obtained greater than 3.7 % CE, using 28 μm droplet and 200 mJ CO_2 laser energy irradiation. These data indicate pre-pulse is very effective to enable high CE no dependence on droplet size in this range.

We have thus demonstrated the possibility to reduce the debris by use of a smaller 20 μm diameter droplet target without degradation in CE. These basic studies, together with theoretical calculations, have contributed to the basic design and development of a high-power production machine capable for further EUV power scaling.

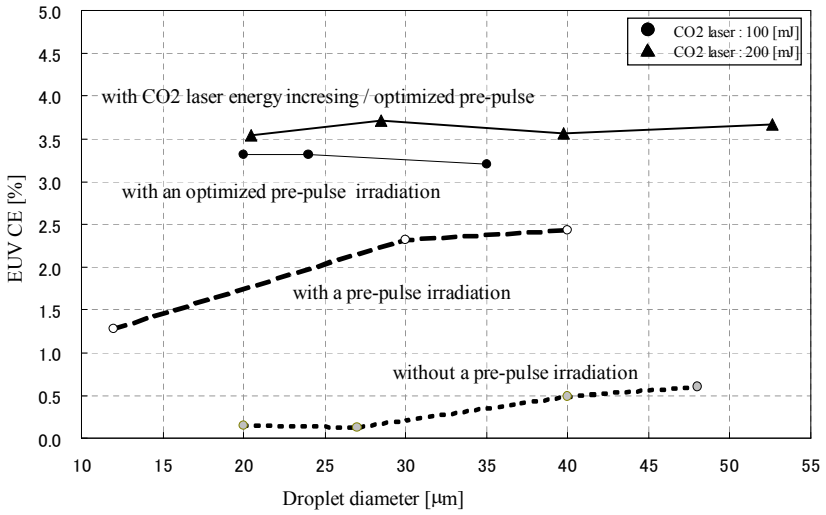

Figure 6: CE as a function of the droplet diameter

Figure 7 shows the EUV clean pulse energy obtained as a function of droplet size and CO_2 laser pulse energy using an optimal pre-pulse laser condition.

Using the small experimental light source tool, and calculating based upon a targeted pulse repetition rate of 100 kHz, we have demonstrated using a 20 μm droplet that 1.55 mJ/pulse EUV pulse energy is achieved (defined as "clean EUV" after filtering out of non-EUV band energy) and therefore >150 W clean EUV power is possible. Further we demonstrated using a 40 μm droplet that 2.52 mJ EUV pulse energy is experimentally observed. Again, calculating for a 100 kHz system, we can demonstrate that >250 W clean EUV power is achievable. It should be noted that with the use of the larger 40 μm droplet, debris increased dramatically compared to the 20 μm Sn droplet case. Therefore, in the future work, we will work further to optimize the 20 μm Sn droplet experiment to target >250 W clean EUV power.

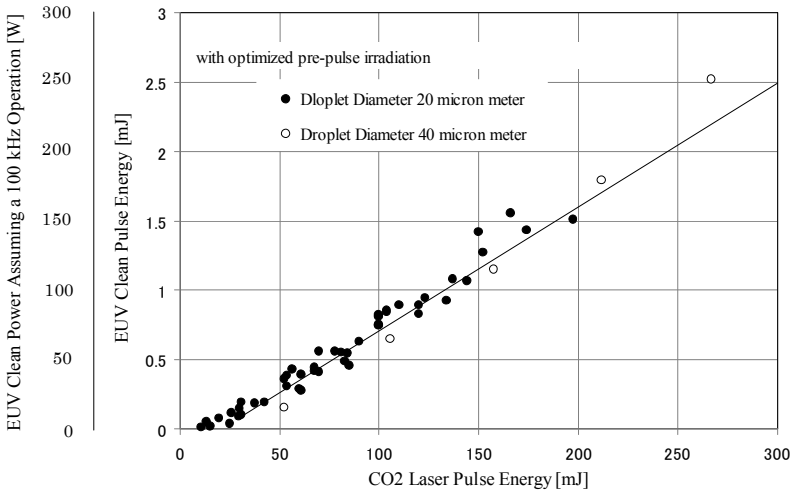

Figure 7: CE as a function of the CO_2 laser pulse energy

3.2 Effective debris mitigation

Our Sn debris mitigation is a simple concept based upon making use of a magnetic field capturing and channeling charged Sn ions away from critical parts of the EUV source system. During the process of EUV plasma creation, obtaining the optimum ratio of the three Sn categories (fragments, neutral atoms, and ions) is important from a debris mitigation perspective. When our double pulse irradiation scheme and small droplets are combined, the majority of Sn ions are able to be trapped as Sn^{n+} within the magnetic field. The ionization rate of Sn will be described the below in this section.

In order to mitigate Sn debris, a pair of superconductive magnetic coils is arranged on opposite sides of the vessel. In reality, however, not all of the Sn atoms and ions can be trapped in the magnetic field. Accordingly, our system is also equipped with a chemical etching mechanism. This chemical etching mechanism is designed to mitigate any remaining Sn atoms that could not have been trapped in the magnetic field and can potentially be deposited on the collector mirror surface or other optically sensitive locations.

The amount and the distribution of the Sn neutral atoms after the pre-pulse laser irradiation in a certain magnetic field were observed with a Laser Induced Fluorescence (LIF) experimental setup [10].

Figure 8 shows the result of the LIF measurements. When there is no main CO_2 laser irradiation, neutral atoms and fragments are observed. With CO_2 laser irradiation, no neutral atoms and fragments are observed.

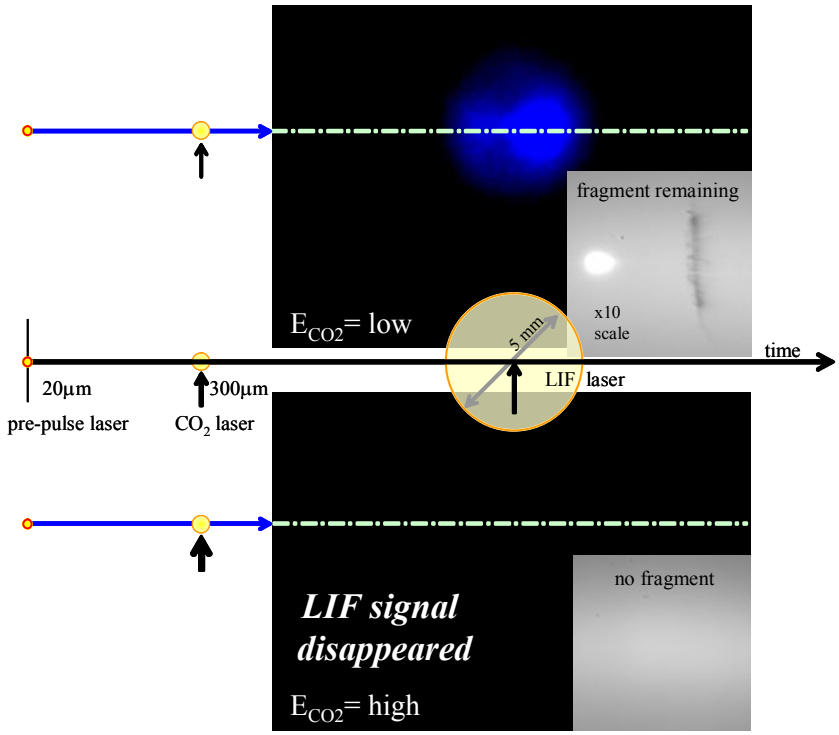

Figure 8: LIF images at pre-pulse with/without pulse CO_2 laser

We conducted two experiments using the LIF metrology setup, with and without CO_2 laser irradiation, and then by comparing the two resultant signals, we are able to conclude 93 % of the Sn atoms are ionized and 7 % of the Sn atoms remain as neutral atoms. This ratio changes with CO_2 laser pulse energy, as shown in Figure 9.

The experimental results indicate when above a certain threshold of CO_2 laser energy, almost all Sn atoms in the droplet are ionized. This is a very positive result, as it indicates the Sn ionization rate remains constant when CO_2 irradiation energy exceeds a definable minimum energy level.

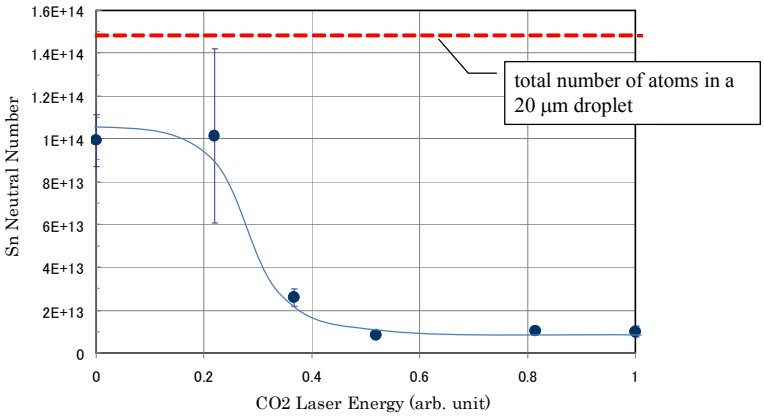

Figure 9: Sn neutral atoms vs. CO_2 laser pulse energy

We measured the ion distribution with the faraday cup measurement [10] with and without a magnetic field. Two faraday cups are set at the position of the collector mirror, where a cup is located in a direction perpendicular to the direction of the magnetic field. The other cup is located where the magnetic flux converges.

Based upon the assumption that the average valence of the Sn ion is two, we calculated the distribution and the collection rate of the ions in the magnetic field. We tested with several magnetic field conditions. Figure 10 also indicates that the Sn ions are collected along the magnetic flux as the magnetic field is enhanced. The collection rate of the ions exceeds 98% under some magnetic field conditions.

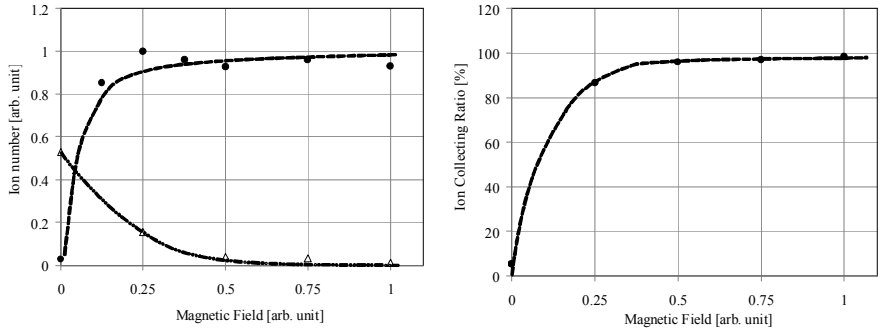

Figure 10: Sn ions collection rate vs. magnetic field strength

The overall results are summarized; we have observed 30 % fragments, 67 % neutral atoms, and 3 % ions from a 20 μm Sn droplet with only pre-pulse laser irradiation. After irradiate CO_2 laser, 0 % of fragments, 7 % of neutral atoms, and 93 % of ions were observed.

3.3 CO_2 laser energy consumption budget

In the previous sections, we discussed Sn behavior during EUV light generation. From the drive laser point of view, we now turn to a discussion of energy transfer from CO_2 laser energy into Sn droplets. In a LPP EUV source, the CO_2 laser energy is either absorbed in the plasma, reflected from the plasma, or transmitted through the plasma. The reflected energy of the CO_2 laser can further be divided into three subcomponents: a) reflection back into the CO_2 laser, b) reflection onto the collector mirror, and c) reflection onto the surrounding vessel wall. Figure 11 graphically shows the defined areas. In order to make an efficient system, it is preferred to maximize the absorbed energy into the Sn and minimize the reflected and transmitted energy. Reducing the reflected energy back into the CO_2 laser will also reduce self-oscillation of the CO_2 laser which could limit the maximum power a drive laser could operate and damage components in the laser system.

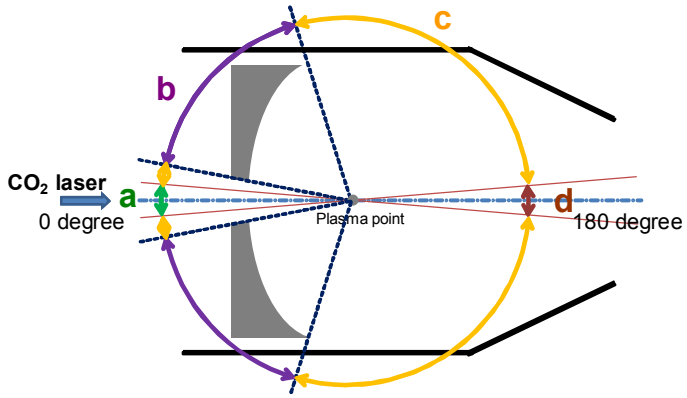

Figure 11: Category of reflected CO_2 laser energy

Figure 12 shows a schematic overview of the test setup, with the power sensors at the measurement positions. The reflected CO_2 laser power distribution can be measured by moving the power sensor (PEM). The transmitted power is measured by a power sensor located at the opposite side of the CO_2 laser inlet. The reflected light towards the CO_2 laser was separated by a beam splitter inside the CO_2 laser beam path.

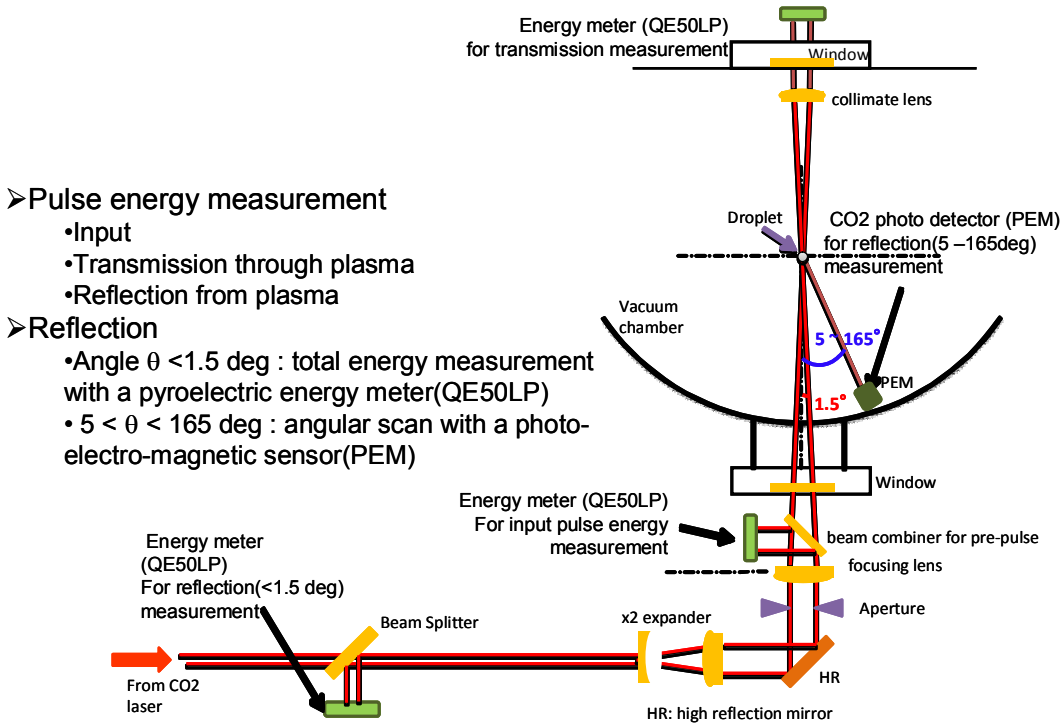

Figure 12: CO_2 laser energy distribution measurement setup

Figure 13, 14 and 15 shows the distributed energy results of 3 experimental tests of the distributed energy with varying pre-pulse energy. The pre-pulse energy of Figure 13 is one fourth of the pre-pulse energy in Figure 15. The pre-pulse energy of Figure 14 is one half of pre-pulse energy in Figure 15. Each category is calculated by fitting a curve through the measured values. Each energy type is integrated within the defined area, as described in Figure 11. The energy distribution is measured in a plane parallel to the CO_2 laser entrance and for calculation purposes the reflected energy is assumed to scatter rotationally symmetric.

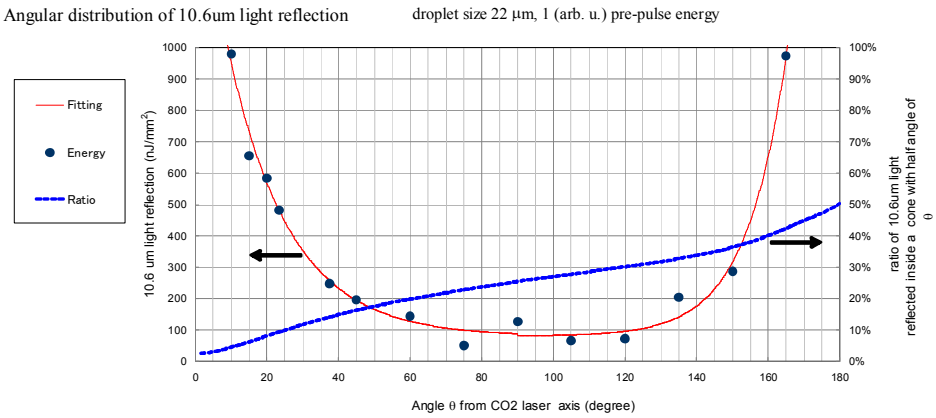

Figure 13: CO_2 laser energy distribution results, 1 (arb. u.) pre-pulse energy

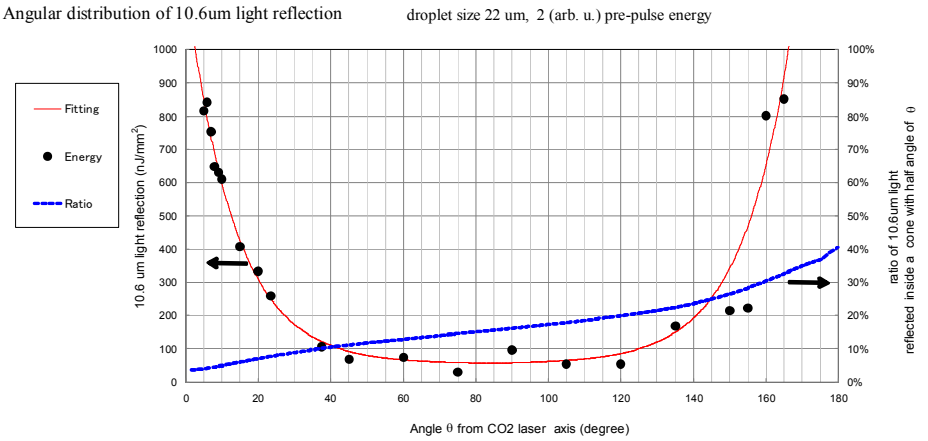

Figure 14: CO_2 laser energy distribution results, 2 (arb. u.) pre-pulse energy

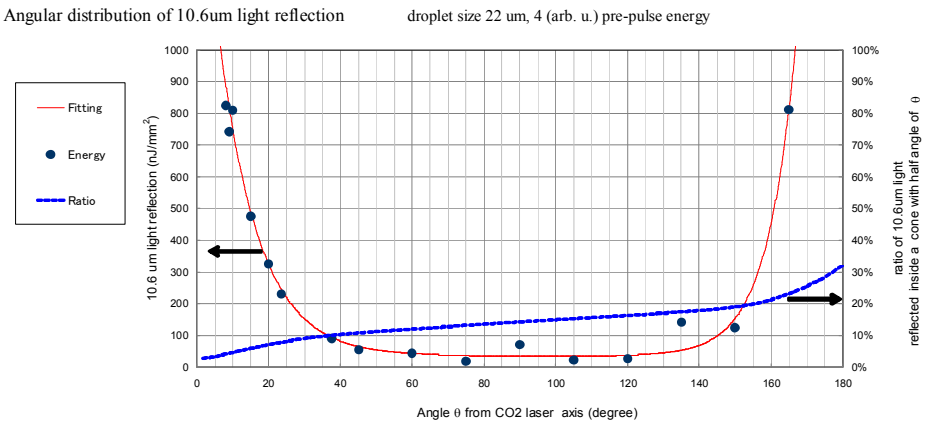

Figure 15: CO_2 laser energy distribution results, 4 (arb. u.) pre-pulse energy

Figure 16 summarizes the results of CO_2 laser energy distribution with varying pre-pulse energy. The CO_2 laser absorption ratio and CE increase with increasing pre-pulse energy. These results demonstrate that higher pre-pulse pulse energy is very effective to maximize CO_2 laser energy absorption into the Sn plasma and minimize transmission and reflection effects. And as expected, another positive aspect of increased pre-pulse pulse energy is increased absorption leading to improved CE.

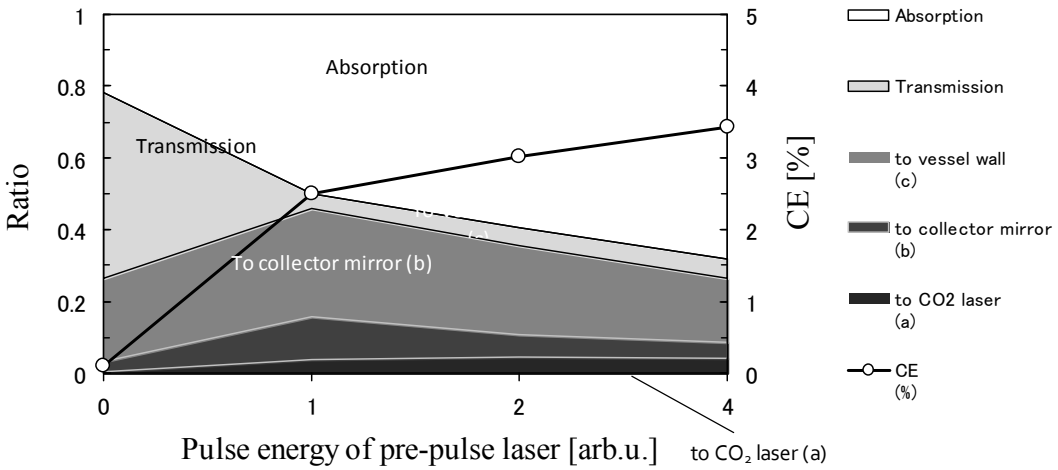

Figure 16: CO_2 laser energy distribution results vs. pre-pulse condition laser energy

CO_2 laser energy power distributions, under optimized conditions, are summarized in Figure 17. The figure shows 68 % absorption, 26.6 % reflected and 5.4 % transmitted CO_2 laser energy power. The 26.6 % reflected power is further broken down to 3.9 % back reflection into the CO_2 laser, 4.6 % towards the collector mirror, and 18.1 % reflected to the vessel walls. In the case of no pre-pulse irradiation, the transmission energy is significantly larger as Sn droplet size (20 μm) and CO_2 laser spot size (300 μm) are not matched. Optimal pre-pulse conditions therefore better match the physical sizes of the Sn mist to the CO_2 beam waist providing very high EUV transmissions with relatively low pre-pulse energies.

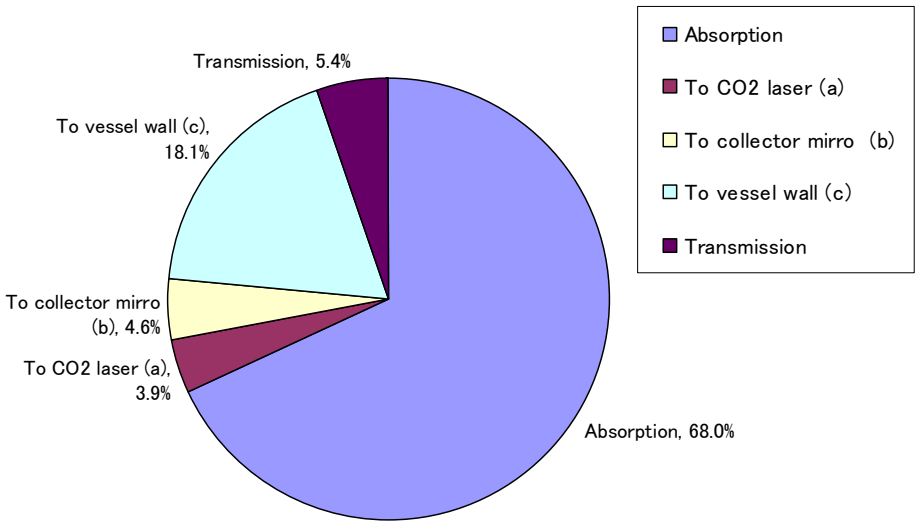

Figure 17: Summary of CO_2 laser energy distribution

4. SUMMARY

In this paper, we have reported results and status from the "small experimental light source tool" and "GL200E proto system".

We have investigated the EUV plasma generation scheme by use of a small experimental tool which operates at 10 Hz. We have proposed a double laser pulse irradiation method to generate LPP plasma efficiently. At this moment we have determined an operation condition demonstrating CE of 3.8 %. And we have obtained 93 % Sn ionization rate when the droplets are irradiated with double laser pulses under proper CO_2 laser pulse conditions. Also the CO_2 laser absorption ratio is up to 68%, reflected CO_2 laser energy back into the CO_2 laser is 3.9 %.

Based on these engineering results from the small experimental tool, we are continuing our development of our first generation EUV light source for HVM: Gigaphoton GL200E. This system implements the following original concepts:

(1) High efficient Sn plasma generation; driven by pulsed CO_2 laser

(2) Double pulse irradiation scheme for Sn plasma generation

(3) Sn debris mitigation by a magnetic field and small Sn droplet size (20 μm)

(4) Hybrid CO_2 laser system using a combination of a short pulse oscillator and commercial cw-CO_2 amplifiers [11]

The design concepts are also reported. These data indicate that our LPP-EUV light source with the magnetic field debris mitigation system will be integrated as the HVM EUVL source system in the near future (Figure 18).

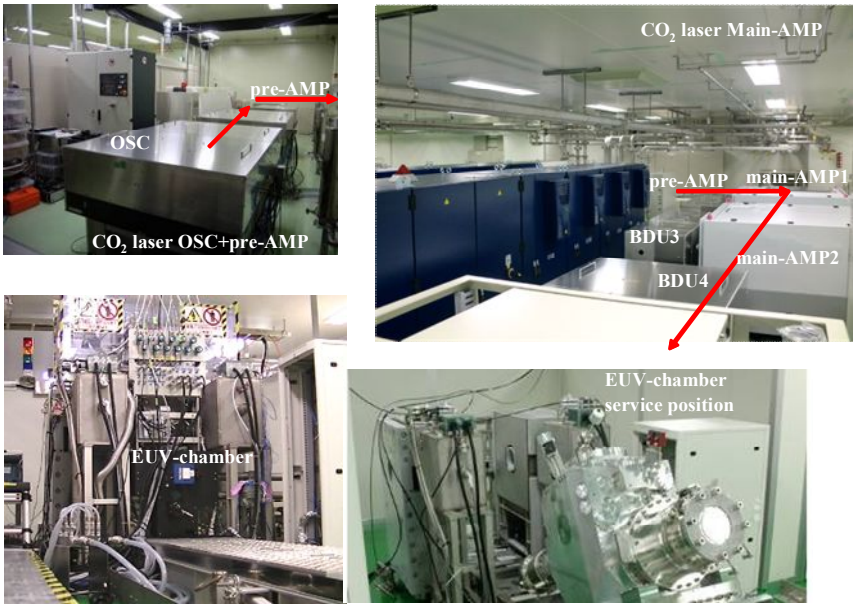

Figure 18: Picture of GL200E system

5. ACKNOWLEDGEMENT

This work was partly supported by the New Energy and Industrial Technology Development Organization (NEDO), JAPAN.

6. REFERENCES

1. Hakaru Mizoguchi, Tamotsu Abe, Yukio Watanabe, Takanobu Ishihara, Takeshi Ohta, Tsukasa Hori, Akihiko Kurosu, Hiroshi Komori, Kouji Kakizaki, Akira Sumitani, Osamu Wakabayashi, Hiroaki Nakarai, Junichi Fujimoto, Akira Endo: ”1st generation Laser-Produced Plasma 100W source system for HVM EUV lithography”, 2010 SEMATECH EUVL Symposium, Kobe, JAPAN (Oct. 17-20, 2010) SO-03.
2. Hakaru Mizoguchi, Tamotsu Abe, Yukio Watanabe, Takanobu Ishihara, Takeshi Ohta, Tsukasa Hori, Akihiko Kurosu, Hiroshi Komori, Kouji Kakizaki, Akira Sumitani, Osamu Wakabayashi, Hiroaki Nakarai, Junichi Fujimoto, and Akira Endo: “First generation laser-produced plasma source system for HVM EUV lithography”, Proc. SPIE 7636, (2010) [7636-08]
3. Hakaru Mizoguchi, Tamotsu Abe, Yukio Watanabe, Takanobu Ishihara, Takeshi Ohta, Tsukasa Hori, Tatsuya Yanagida, Hitosh Nagano, Takayuki Yabu, Shinji Nagai, Georg Soumagne, Akihiko Kurosu, Krzysztof M. Nowak, Takashi Suganuma, Masato Moriya, Kouji Kakizaki, Akira Sumitani, Hidenobu Kameda, Hiroaki Nakarai, Junichi Fujimoto: “100W 1st Generation Laser-Produced Plasma light source system for HVM EUV lithography”, Proc. SPIE 7969 (2011) [796908]
4. Junichi Fujimoto, Toru Suzuki, Hiroaki Nakarai, Tsukasa Hori, Satoshi Tanaka, Yukio Watanabe, Yasufumi Kawasuji, Takeshi Ohta, Tamotsu Abe, Hakaru Mizoguchi, “Development of LPP-EUV Source for HVM EUVL”, 2011 International Symposium on Extreme Ultraviolet Lithography (2011)
5. Tsukasa Hori, Tatsuya Yanagida, Takayuki Yabu, Hitoshi Nagano, Georg Soumagne, Kouji Kakizaki, Akira Sumitani, Junichi Fujimoto, Hakaru Mizoguchi: ”Investigation on high conversion efficiency and Tin debris mitigation for laser produced plasma EUV light source”, 2010 SEMATECH EUVL Symposium, Kobe, JAPAN (2010.Oct. 17-20) SO-04.
6. Tatsuya Yanagida, Hitoshi Nagano, Yasunori Wada, Takayuki Yabu, Shinji Nagai, Georg Soumagne, Tsukasa Hori, Kouji Kakizaki, Akira Sumirani, Junichi Fujimoto, Hakaru Mizoguchi, Akira Endo: “Characterization and optimization of tin particle mitigation and EUV conversion efficiency in a laser produced plasma EUV light source”, Proc. SPIE 7969 (2011) [7969-100]
7. K. Nishihara, A. Sasaki, A. Sunahara, and T. Nishikawa, EUV Sources for Lithography, Chap. 11, ed. V. Bakshi, SPIE, Bellingham, 2005.
8. H. Tanaka, A. Matsumoto, K. Akinaga, A. Takahashi, and T. Okada: “Comparative study on emission characteristics of extreme ultraviolet radiation from CO_2 and Nd:YAG laser-produced tin plasmas”, Appl. Phys. Lett. 87, 041503 (2005)
9. H. Hoshino, T. Suganuma, T. Asayama, K. Nowak, M. Moriya, T. Abe, A. Endo, A. Sumitani: “LPP EUV light source employing high-power CO_2 laser”, Proc. SPIE 6921 (2008) [6921-31]
10. Yoshifumi Ueno, Hideo Hoshino, Tatsuya Ariga, Taisuke Miura, Masaki Nakano, Hiroshi Komori, Georg Soumagne, Akira Endo, Hakaru Mizoguchi, Akira Sumitani and Koichi Toyoda: “Characterization of Various Sn Targets with Respect to Debris and Fast Ion Generation”, Proc. SPIE 6517 (2007) [6517-123]
11. Junichi Fujimoto, Takeshi Ohta, Krzysztof M. Nowak, Takashi Suganuma, Hidenobu Kameda, Masato Moriya, Toshio Yokoduka, Kouji Fujitaka, Akira Sumitani, Hakaru Mizoguchi: “Development of the reliable 20 kW class pulsed carbon dioxide laser system for LPP EUV light source”, Proc. SPIE 7969 (2011) [7969-99]